Inorganic Chemistry
Article

Inorg. Chem. **2010**, *49*, 11009–11017 **11009**
DOI: 10.1021/ic1014785

Photoenhanced Oxidative DNA Cleavage with Non-Heme Iron(II) Complexes

Qian Li, Wesley R. Browne,* and Gerard Roelfes*

Stratingh Institute for Chemistry, University of Groningen, Nijenborgh 4, 9747AG Groningen, The Netherlands

Received July 23, 2010

The DNA cleavage activity of iron(II) complexes of a series of monotopic pentadentate *N*,*N*-bis(2-pyridylmethyl)-*N*-bis(2-pyridyl)methylamine (N4Py)-derived ligands (**1**−**5**) was investigated under laser irradiation at 473, 400.8, and 355 nm in the absence of a reducing agent and compared to that under ambient lighting. A significant increase in activity was observed under laser irradiation, which is dependent on the structural characteristics of the complexes and the wavelength and power of irradiation. Under photoirradiation at 355 nm, direct double-stand DNA cleavage activity was observed with Fe^{II}-**1** and Fe^{II}-**3**−**5**, and a 56-fold increase in the single-strand cleavage activity was observed with Fe^{II}-**2**. Mechanistic investigations revealed that $O_2^{\bullet-}$, $^1O_2$, and $OH^{\bullet}$ contribute to the photoenhanced DNA cleavage activity, and that their relative contribution is dependent on the wavelength. It is proposed that the origin of the increase in activity is the photoenhanced formation of an $Fe^{III}OOH$ intermediate as the active species or precursor.

Introduction

The design of compounds capable of affecting efficient cleavage of DNA is of great interest because of their potential importance for the development of new antitumor drugs. A subclass of DNA cleaving agents are the metal complexes based on transition metals such as iron, copper, zinc, nickel, rhodium, and the lanthanides.[1−8] Important representatives of this class are the metal complexes of natural ligands, such as bleomycins (BLMs). The antitumor activity of BLMs, which are clinically used in the treatment of, e.g., cancers of the cervix, head, and neck and testicular cancers, relies on the ability of the corresponding metal complexes to mediate oxidative DNA scission involving both single- and double-strand DNA cleavage.[1,9−12] Compared to single-strand DNA cleavage (ssc), the repair of double-strand DNA cleavage (dsc) by cellular repair mechanisms is much less efficient; therefore, dsc is believed to be the major source of cytotoxicity of metallobleomycins.[13,14]

The mechanisms of BLM activation and subsequent DNA oxidation have been extensively investigated in the presence of metal ions and O_2.[1] Many model complexes for metallobleomycins have been developed as synthetic DNA cleaving agents and have proven to be capable of cleaving DNA in the presence of O_2, albeit that they generally possess low to moderate activity and induce ssc only.[8,15] In our group, the pentadentate ligand *N*,*N*-bis(2-pyridylmethyl)-*N*-bis(2-pyridyl)-methylamine (N4Py, **1**; Chart 1) was designed and synthesized as a mimic of the metal-binding domain of BLMs.[16] Its iron(II) complex is capable of inducing DNA strand breaks efficiently with molecular oxygen as the terminal oxidant, even in the absence of an external reducing agent.[16b] Recently, we have reported two examples of mononuclear Fe^{II}N4Py complexes capable of inducing direct double-strand cleavage, albeit to a lesser extent than with the analogous multinuclear

*To whom correspondence should be addressed. E-mail: W.R.Browne@rug.nl (W.R.B.), J.G.Roelfes@rug.nl (G.R.). Fax: +31 50 3634296.

(1) (a) Burger, R. M. *Chem. Rev.* **1998**, *98*, 1153–1170. (b) Claussen, C. A.; Long, E. C. *Chem. Rev.* **1999**, *99*, 2797–2816.
(2) Armitage, B. *Chem. Rev.* **1998**, *98*, 1171–1200.
(3) Clarke, M. J.; Zhu, F.; Frasca, D. R. *Chem. Rev.* **1999**, *99*, 2511–2534.
(4) Marnett, L. J. *Carcinogenesis* **2000**, *21*, 361–370.
(5) Cowan, J. A. *Curr. Opin. Chem. Biol.* **2001**, *5*, 634–642.
(6) Wolkenberg, S. E.; Boger, D. L. *Chem. Rev.* **2002**, *102*, 2477–2496.
(7) Jiang, Q.; Xiao, N.; Shi, P.; Zhu, Y.; Guo, Z. *Coord. Chem. Rev.* **2007**, *251*, 1951–1972.
(8) Pitié, M.; Pratviel, G. *Chem. Rev.* **2010**, *110*, 1018–1059.
(9) Umezawa, H.; Maeda, K.; Takeuchi, T.; Okami, Y. *J. Antibiot.* **1966**, *19*, 200–209.
(10) Hecht, S. M. *Bleomycin: Chemical, Biochemical and Biological Aspects*; Springer: New York, 1979.
(11) Pogozelski, W. K.; Tullius, T. D. *Chem. Rev.* **1998**, *98*, 1089–1108.
(12) Hecht, S. M. *J. Nat. Prod.* **2000**, *63*, 158–168.
(13) (a) Stubbe, J.; Kozarich, J. W.; Wu, W.; Vanderwall, D. E. *Acc. Chem. Res.* **1996**, *29*, 322–330. (b) Chen, J.; Stubbe, J. *Nat. Rev. Cancer* **2005**, *5*, 102–112. (c) Thompson, L.; Limoli, C.; Origin, C. *Recognition, Signaling and Repair of DNA Double Strand in Mammalian Cells*; Springer: New York, 2003.
(14) Petering, D. H.; Byrnes, R. W.; Antholine, W. E. *Chem. Biol. Interact.* **1990**, *73*, 133–182.
(15) (a) Hertzberg, R. P.; Dervan, P. B. *J. Am. Chem. Soc.* **1982**, *104*, 313–315. (b) Hertzberg, R. P.; Dervan, P. B. *Biochemistry* **1984**, *23*, 3934–3945. (c) Sigman, D. S.; Mazumder, A.; Perrin, D. M. *Chem. Rev.* **1993**, *93*, 2295–2316. (d) Guajardo, R. J.; Hudson, S. E.; Brown, S. J.; Mascharak, P. K. *J. Am. Chem. Soc.* **1993**, *115*, 7971–7977. (e) Silver, G. C.; Trogler, W. C. *J. Am. Chem. Soc.* **1995**, *117*, 3983–3993. (f) Pratviel, G.; Bernadou, J.; Meunier, B. *Angew. Chem., Int. Ed.* **1995**, *34*, 746–769. (g) Mialane, P.; Nivorojkine, A.; Pratviel, G.; Azéma, L.; Slany, M.; Godde, F.; Simaan, A.; Banse, F.; Kargar-Grisel, T.; Bouchoux, G.; Sainton, J.; Horner, O.; Guilhem, J.; Tchertanova, L.; Meunier, B.; Girerd, J. J. *Inorg. Chem.* **1999**, *38*, 1085–1092. (h) Marchand, C.; Nguyen, C. H.; Ward, B.; Sun, J. S.; Bisagni, E.; Garestier, T.; Hélène, C. *Chem.—Eur. J.* **2000**, *6*, 1559–1563. (i) Hemmert, C.; Pitié, M.; Renz, M.; Gornitzka, H.; Soulet, S.; Meunier, B. *J. Biol. Inorg. Chem.* **2001**, *6*, 14–22. (j) Wong, E. L.; Fang, G.; Che, C.; Zhu, N. *Chem. Commun.* **2005**, 4578–4580.

Published on Web 11/08/2010

Chart 1. Monotopic N4Py Ligands Employed in the Study

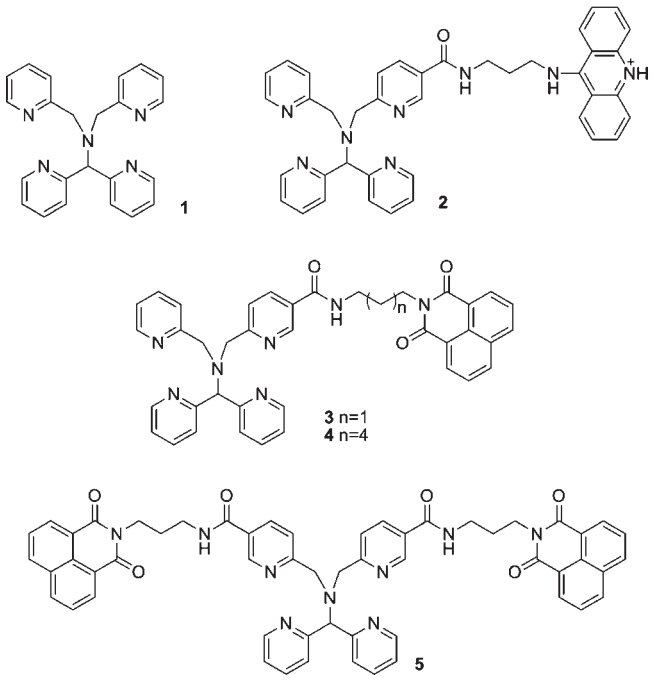

complexes.[16f] Covalent attachment of DNA binders such as 9-aminoacridine, an ammonium group, or 1,8-naphthalimide to the N4Py ligand gave rise to increased DNA cleavage activity in the presence of dithiothreitol (DTT).[16f] In contrast, in the absence of a reducing agent, no beneficial effect of the covalently attached DNA binding moieties was observed. This was attributed to the reduction from Fe^{III} to Fe^{II}, which is required for oxygen activation, being rate-limiting in the absence of a reductant. Mechanistic investigations have revealed the important role played by superoxide radicals, and the proposed mechanism involves the formation of an $Fe^{III}OOH$ intermediate as the active species or precursor.[16f]

The DNA binding moieties that were employed, i.e., 9-aminoacridine and naphthalimide derivatives, are well-known photosensitizers and have been demonstrated to be capable of inducing photocleavage of DNA via electron transfer and the resultant formation of reactive oxygen species (ROS).[17] It was envisioned that mononuclear Fe^{II}N4-Py complexes with a covalently attached 9-aminoacridine or 1,8-naphthalimide moiety would give rise to enhanced DNA cleavage activity under photoirradiation. Whereas extensive studies have focused on DNA photocleavage by organic compounds and metal complexes,[2,17−19] in particular rhodium and ruthenium complexes,[19] iron complexes are underrepresented in this aspect.[20]

Here, we present the results of a study of the effect of irradiation with light of various wavelengths on the DNA cleavage activity of the iron(II) complexes of a series of monotopic N4Py ligands (Chart 1) under aerobic conditions in the absence of reducing reagents. The mechanism of the DNA cleavage process induced by the parent complex Fe^{II}-**1** under photoirradiation was investigated by inclusion of a series of mechanistic probes in the reaction mixture.

Experimental Section

Materials and Instrumentation. All reagents and solvents were used as purchased without further purification unless noted otherwise. Ligands **1**−**5** were synthesized according to literature procedures, and all data are in agreement with those reported.[16a,b,f] UV−vis spectra were recorded using 1- or 5-cm path-length quartz cells on a Jasco V-660 spectrophotometer. Absorption maxima are ±2 nm; molar absorptivities are ±5%. Corrected fluorescence excitation and emission spectra were recorded in 10-mm path-length cells on a Jasco FP-6200 spectrofluorimeter. All spectra were recorded at 20 °C. Photoirradiation was performed by using continuous-wave (CW) lasers (473 nm, 100 mW at source, Cobolt; 400.8 nm, 50 mW at source, Power-Technology; 355 nm, 10 mW at source, Cobolt) and pulsed lasers (355 nm, 6−8 ns, 10 Hz, Spitlight 200, Innolas). The power of laser excitation at the sample was calculated using the quantum counter ferrioxalate and verified using a power sensor (PM10 V1, with a FieldMate Laser Power Meter, Coherent).

pUC18 plasmid DNA, isolated from *Escherichia coli* XL1 Blue, was purified using QIAGEN maxi kits. Concentrations were determined by UV−vis spectrometry at 260 nm using a NanoDrop 1000 spectrophotometer (Thermo Scientific). Restriction enzymes and restriction buffers were purchased from New England Biolabs. A DNA ladder (SmartLadder, 0.2−10 kbp) was purchased

(16) (a) Lubben, M.; Meetsma, A.; Wilkinson, E. C.; Feringa, B. L.; Que, L., Jr. *Angew. Chem., Int. Ed. Engl.* **1995**, *34*, 1512–1514. (b) Roelfes, G.; Branum, M. E.; Wang, L.; Que, L., Jr.; Feringa, B. L. *J. Am. Chem. Soc.* **2000**, *122*, 11517–11518. (c) Roelfes, G.; Vrajmasu, V.; Chen, K.; Ho, R. Y. N.; Rohde, J.; Zondervan, C.; la Crois, R. M.; Schudde, E. P.; Lutz, M.; Spek, A. L.; Hage, R.; Feringa, B. L.; Münck, E.; Que, L., Jr. *Inorg. Chem.* **2003**, *42*, 2639–2653. (d) van den Berg, T. A.; Feringa, B. L.; Roelfes, G. *Chem. Commun.* **2007**, 180–182. (e) Megens, R. P.; van den Berg, T. A.; de Bruijn, A. D.; Feringa, B. L.; Roelfes, G. *Chem.—Eur. J.* **2009**, *15*, 1723–1733. (f) Li, Q.; van den Berg, T. A.; Feringa, B. L.; Roelfes, G. *Dalton Trans.* **2010**, *39*, 8012–8021.

(17) For examples, see:(a) Buchardt, O.; Egholm, M.; Karup, G.; Nielsen, P. E. *J. Chem. Soc., Chem. Commun.* **1987**, 1696–1697. (b) Nielsen, P. E.; Jeppesen, C.; Egholm, M.; Buchardt, O. *Nucleic Acids Res.* **1988**, *16*, 3877–3888. (c) Saito, I.; Takayama, M.; Kawanishi, S. *J. Am. Chem. Soc.* **1995**, *117*, 5590–5591. (d) Aveline, B. M.; Matsugo, S.; Redmond, R. W. *J. Am. Chem. Soc.* **1997**, *119*, 11785–11795. (e) Rogers, J. E.; Abraham, B.; Rostkowski, A.; Kelly, L. A. *Photochem. Photobiol.* **2001**, *74*, 521–531. (f) Da Ros, T.; Spalluto, G.; Boutorine, A. S.; Bensasson, R. V.; Prato, M. *Curr. Pharm. Des.* **2001**, *7*, 1781–1821. (g) Joseph, J.; Eldho, N. V.; Ramaiah, D. *Chem.—Eur. J.* **2003**, *9*, 5926–5935. (h) Xu, Y.; Huang, X.; Qian, X.; Yao, W. *Bioorg. Med. Chem.* **2004**, *12*, 2335–2341. (i) Fernández, M.-J.; Wilson, B.; Palacios, M.; Rodrigo, M.-M.; Grant, K. B; Lorente, A. *Bioconjugate Chem.* **2007**, *18*, 121–129.

(18) For examples, see:(a) McMillin, D. R.; McNett, K. M. *Chem. Rev.* **1998**, *98*, 1201–1220. (b) Ali, H.; van Lier, J. E. *Chem. Rev.* **1999**, *99*, 2379–2450. (c) Teulade-Fichou, M.-P.; Perrin, D.; Boutorine, A.; Polverari, D.; Vigneron, J.-P.; Lehn, J.-M.; Sun, J.-S.; Garestier, T.; Hélène, C. *J. Am. Chem. Soc.* **2001**, *123*, 9283–9292. (d) Szaciowski, K.; Macyk, W.; Drzewiecka-Matuszek, A.; Brindell, M.; Stochel, G. *Chem. Rev.* **2005**, *105*, 2647–2694. (e) Roy, M.; Pathak, B.; Patra, A. K.; Jemmis, E. D.; Nethaji, M.; Chakravarty, A. R. *Inorg. Chem.* **2007**, *46*, 11122–11132. (f) Ishikawa, Y.; Yamakawa, N.; Uno, T. *Bioorg. Med. Chem.* **2007**, *15*, 5230–5238. (g) Kumar, A.; Sevilla, M. D. *Chem. Rev.* **2010**, DOI: 10.1021/cr100023g

(19) For recent examples, see:(a) Chifotides, H. T.; Dunbar, K. R. *Acc. Chem. Res.* **2005**, *38*, 146–156. (b) Elias, B.; Kirsch-De Mesmaeker, A. *Coord. Chem. Rev.* **2006**, *250*, 1627–1641. (c) Jain, A.; Wang, J.; Mashack, E. R.; Winkel, B. S. J.; Brewer, K. J. *Inorg. Chem.* **2009**, *48*, 9077–9084. (d) Ernst, R. J.; Song, H.; Barton, J. K. *J. Am. Chem. Soc.* **2009**, *131*, 2359–2366. (e) Aguirre, J. D.; Angeles-Boza, A. M.; Chouai, A.; Pellois, J.-P.; Turro, C.; Dunbar, K. R. *J. Am. Chem. Soc.* **2009**, *131*, 11353–11360. (f) Joyce, L. E.; Aguirre, J. D.; Angeles-Boza, A. M.; Chouai, A.; Fu, P. K.-L.; Dunbar, K. R.; Turro, C. *Inorg. Chem.* **2010**, *49*, 5371–5376. (g) Sun, Y.; Joyce, L. E.; Dickson, N. M.; Turro, C. *Chem. Commun.* **2010**, 2426–2428.

(20) (a) Maurer, T. D.; Kraft, B. J.; Lato, S. M.; Zaleski, J. M.; Ellington, A. D. *Chem. Commun.* **2000**, 69–70. (b) Mohler, D. L.; Barnhardt, E. K.; Hurley, A. L. *J. Org. Chem.* **2002**, *67*, 4982–4984. (c) Wilson, B.; Gude, L.; Fernández, M.; Lorente, A.; Grant, K. B. *Inorg. Chem.* **2005**, *44*, 6159–6173. (d) Mukherjee, A.; Dhar, S.; Nethaji, M.; Chakravarty, A. R. *Dalton Trans.* **2005**, 349–353. (e) Roy, M.; Bhowmick, T.; Santhanagopal, R.; Ramakumar, S.; Chakravarty, A. R. *Dalton Trans.* **2009**, 4671–4682. (f) Saha, S.; Majumdar, R.; Roy, M.; Dighe, R. R.; Chakravarty, R. R. *Inorg. Chem.* **2009**, *48*, 2652–2663. (g) Begum, M. S. A.; Saha, S.; Nethaji, M.; Chakravarty, A. R. *J. Inorg. Biochem.* **2010**, *104*, 477–484.

from Eurogentec. Catalase (from bovine liver) and superoxide dismutase (SOD; from bovine erythrocytes) were purchased from Sigma-Aldrich. Agarose used for gel electrophoresis was purchased from Invitrogen. Pictures of the gel slabs were taken with a Spot Insight CCD camera using the software program *Spot*, version 3.4. The intensity of the bands on the film was quantified by using the software program *Gel-Pro Analyzer*, version 4.0. Statistical calculations were performed using *Mathematica*, version 7.01.

Determination of the Irradiation Power and Photo Flux. The iron(III) oxalate/phenanthroline actinometer system was used to determine the light flux (R) of irradiation.[21] The power (P) at the sample was calculated using eq 1, in which E_p is the energy of one photon, h is Plank's constant (6.626×10^{-34} J s), c is the speed of light (3.0×10^8 m s^{-1}), and λ is the wavelength of the light source (473, 400.8, and 355 nm). The values of power determined by actinometry are in good agreement with that measured using the power sensor. Detailed information of the actinometry is provided as Supporting Information.

$$P = E_p R = \frac{\hbar c}{\lambda} R \tag{1}$$

Quantum yields of fluorescence, Φ_f, were determined using 9-methylanthracene, $\Phi_f = 0.27$ in ethanol, as a reference.[21] Details of Φ_f measurements are provided as Supporting Information.

DNA Cleavage Experiments. Iron(II) complexes of ligands **1** and **2** were dissolved in H_2O. A total of 1 equiv of $(NH_4)_2Fe^{II}(SO_4)_2 \cdot 6H_2O$ was added to solutions of ligands **1** and **3**−**5** in H_2O to generate the corresponding iron(II) complexes in situ. *N*, *N*-Dimethylformamide [DMF; 1% (v/v)] was used to aid the dissolution of ligands **3**−**5** in H_2O. The respective iron(II) complex solutions were added to a buffered solution (10 mM Tris-HCl, pH 8.0) of supercoiled pUC18 plasmid DNA in 1.5 mL eppendorfs. The reaction solutions, with a final volume of 50 μL and a final concentration of 1.0 μM iron(II) complex, 0.1 μg μL^{-1} DNA (150 μM in base pairs), were incubated at 37 °C in the dark or under laser irradiation with 473, 400.8, or 355 nm light. Details of the experimental setup are provided as Supporting Information.

Samples (2 μL) were taken from the irradiated reaction solutions at the time points indicated, quenched by addition to 15 μL of a NaCN solution (1 mg mL^{-1}, containing 2040 equiv of NaCN with respect to Fe^{II}N4Py) with 3 μL of a loading buffer (consisting of 0.08% bromophenol blue and 40% sucrose, 6× concentrated), and immediately frozen in liquid nitrogen. The samples were run on 1.2% agarose gels in a 1× concentrated Tris-acetate-EDTA buffer for at least 90 min at 70 V. Gels were stained in an ethidium bromide (EtBr) bath (1.0 μg mL^{-1}) for 45 min and then washed with a gel running buffer. Quantification was performed by fluorescence imaging, and a correction factor of 1.31 was used to compensate for the reduced EtBr uptake capacity of supercoiled plasmid pUC18 DNA.[16d] All data are an average of cleavage experiments that were performed at least in triplicate.

Quantification of ssc and dsc. The average numbers of single- (n) and double-strand (m) cuts in a DNA molecule were calculated using both eqs 2 and 3, in which f_{III} and f_I are fractions of linear DNA and supercoiled DNA, respectively.[22c] Equation 4 is the Freifelder−Trumbo relationship,[22a] in which h is the maximum distance in base pairs between nicks on opposite strands to generate a double-strand cut (i.e., 16) and L is the total number of base pairs of DNA used (2686 bp for pUC18 plasmid DNA). Uncertainties in the values of m and n were calculated by a Monte Carlo simulation as described previously.[16d−f]

$$f_{III} = m e^{-m} \tag{2}$$

$$f_I = e^{-(m+n)} \tag{3}$$

$$m = \frac{n^2(2h+1)}{4L} \tag{4}$$

Calculation of Cleavage Rate. In the case of a pure ssc process, the average numbers of single-strand cuts per DNA molecule (n) at different time points were calculated by using eq 5 (when linear DNA is not present) and eq 6 (when linear DNA is present). Uncertainty limits of the data were calculated based on a Monte Carlo simulation, taking into account a standard deviation of $\sigma = 0.03$ for individual DNA fractions.[23] The calculated values of n can be plotted as a function of time, and the rate constant (k_{obs}) of ssc was determined from the linear fit of the graph.[16f] Values of k_{obs} are corrected to k^* by using eq 7, taking into account the concentrations of DNA (0.1 μg μL^{-1} and 0.0564 μM) and the iron(II) complexes (1.0 μM).

$$f_I = e^{-n} \tag{5}$$

$$f_I + f_{II} = [1 - n(2h+1)/2L]^{n/2} \tag{6}$$

$$k^* = k_{obs}\frac{[\text{DNA}]}{[\text{complex}]} \tag{7}$$

Table 1. Electronic Absorption Data for Iron(II) Complexes of Ligands **1**−**5**[a]

complex	absorption λ_{max}/nm (ε/10^4 M^{-1} cm^{-1})
Fe^{II}-**1**	382 (0.21), 455 (0.12)
Fe^{II}-**2**	390 (sh), 413 (1.11), 434 (0.95), 500 (sh)
Fe^{II}-**3**[b]	345 (1.29), 455 (sh)
Fe^{II}-**4**[b]	345 (0.66), 455 (sh)
Fe^{II}-**5**[b]	330 (3.76), 455 (sh)

[a] The absorption spectra were recorded in aqueous solution in 10 mM Tris-HCl (pH 8.0) at 20 °C (Figure S3 in the Supporting Information). [b] 1% (v/v) DMF was used to aid ligand dissolution.

Results and Discussion

The ligands employed in the present study are shown in Chart 1. The ligands **1**−**5** and their corresponding iron(II) complexes were prepared and characterized following previously reported procedures.[16a,b,f]

UV−vis spectral data for the mononuclear Fe^{II}N4Py complexes in 10 mM Tris-HCl buffer (pH 8.0) are listed in Table 1. The absorption maxima of Fe^{II}-**1** are observed at 382 and 455 nm. In the case of the iron(II) complexes of ligands **2** and **3**−**5**, the absorption maximum of the Fe^{II}N4Py core overlaps with the absorptions of the 9-aminoacridine and 1,8-naphthalimide moiety, respectively (Figure S3 in the Supporting Information). It is notable that the addition of 1 equiv of Fe^{2+} caused the absorption band of ligand **5** to broaden and blue-shift by ca. 10 nm, with a concomitant increase in the intensity of the absorption maximum at 340 nm, which strongly suggests the formation of aggregates (vide infra).

On the basis of the UV−vis absorption spectra of the iron(II) complexes of ligands **1**−**5**, the wavelengths 355, 400.8, and 473 nm were selected for photoirradiation in the DNA cleavage study. Both CW and pulsed lasers were employed.

(21) Montalti, M.; Credi, A.; Prodi, L.; Gandolfi, M. T. *Handbook of Photochemistry*, 3rd ed.; CRC Press: Boca Raton, FL, 2006.

(22) (a) Freifelder, D.; Trumbo, B. *Biopolymers* **1969**, *7*, 681–693. (b) Cowan, R.; Collis, C. M.; Grigg, G. W. *J. Theor. Biol.* **1987**, *127*, 229–243. (c) Povirk, L. F.; Wübker, W.; Köhnlein, W.; Hutchinson, F. *Nucleic Acids Res.* **1977**, *4*, 3573–3580.

(23) The standard deviation was determined independently by 24 identical DNA oxidation experiments with Fe^{II}-**1**, and 0.03 is the largest value of the standard deviation in the experiments. See ref 16d for details.

Table 2. DNA Cleavage under Ambient Lighting and Photoirradiation[a]

			nicked DNA (%)				linear DNA (%)
entry	cleaving agent	time (min)	ambient lighting[b]	473 nm[b] (30.3 mW)	400.8 nm[b] (17.4 mW)	355 nm[c] (24.6 mW)	355 nm[c] (24.6 mW)
1		90	0	0	0	16 ± 3	0
2	Fe^{II}-**1**	10	7 ± 1	19 ± 2	18 ± 2	75 ± 1	3 ± 1
		90	22 ± 2	48 ± 1	58 ± 1	80 ± 1	13 ± 1
3	Fe^{II}-**2**	10	7 ± 1	10 ± 2	16 ± 4	63 ± 4	0
		90	29 ± 2	55 ± 2	80 ± 3	100	
4	Fe^{II}-**3**	10	5 ± 1	6 ± 1	7 ± 1	56 ± 3	1 ± 1
		90	18 ± 1	32 ± 1	31 ± 5	75 ± 2	19 ± 1
5	Fe^{II}-**4**	10	3 ± 2	8 ± 1	12 ± 2	42 ± 4	0
		90	8 ± 2	36 ± 2	41 ± 3	75 ± 1	15 ± 2
6	Fe^{II}-**5**	10	2 ± 1	2 ± 1	3 ± 1	43 ± 6	1 ± 1
		90	4 ± 1	9 ± 1	15 ± 3	72 ± 5	17 ± 3

[a] 1 μM iron complex, 0.1 μg μL^{-1} supercoiled pUC18 DNA (150 μM bp), 10 mM Tris-HCl buffer (pH 8.0), 37 °C. A correction factor of 1.31 is used for the reduced EtBr uptake capacity of supercoiled plasmid pUC18 DNA.[16d] The limit for accurate quantification is exceeded when more than 37% linear DNA was formed. [b] Only nicked DNA was formed. [c] Besides nicked DNA, linear DNA was also formed.

Table 3. Control Experiments of DNA Cleavage[a]

			nicked DNA (%)		
no.	reagents	time (min)	ambient lighting	400.8 nm (1.2 mW)	355 nm (2.6 mW)
1	$(NH_4)_2Fe^{II}(SO_4)_2 \cdot 6H_2O$	30	0	2 ± 2	5 ± 3
2	**1**	30	0	0	1 ± 1
3	$(NH_4)_2Fe^{II}(SO_4)_2 \cdot 6H_2O$ + **1**	30	18 ± 3	43 ± 2	41 ± 10
4	Fe^{II}-**1**	30	14 ± 1	37 ± 5	47 ± 12
5	9-aminoacridine	30	0	5 ± 3	2 ± 2
6	1,8-naphthalimide	30	0	0	15 ± 2

[a] 1 μM reagent, 0.1 μg μL^{-1} supercoiled pUC18 DNA (150 μM bp), Tris-HCl buffer (pH 8.0), 37 °C. A correction factor of 1.31 is used for the reduced EtBr uptake capacity of supercoiled plasmid pUC18 DNA.

The DNA cleavage activities of the iron(II) complexes of ligands **1**−**5** were investigated in the cleavage of supercoiled pUC18 (0.1 μg μL^{-1}, 150 μM bp) in 10 mM Tris-HCl buffer (pH 8.0) at 37 °C in the absence of any external reductants within 90 min under laser irradiation at 473, 400.8, and 355 nm, respectively. The final concentration of the cleaving agents was 1 μM based on iron(II), with a stoichiometry of 1:150 with respect to DNA base pairs. All of the experiments were carried out at least in triplicate independently.

Effect of Photoirradiation on DNA Cleavage. Table 2 and Figures S4−S6 in the Supporting Information show the time dependence of DNA cleavage with iron(II) complexes of ligands **1**−**5** under photoirradiation with a light flux of 7.2×10^{16} photons s^{-1} (CW 473 nm, 30.3 mW), 3.5×10^{16} photons s^{-1} (CW 400.8 nm, 17.4 mW), and 4.4×10^{16} photons s^{-1} (pulsed 355 nm, 24.6 mW), respectively. To facilitate comparison, the results under normal ambient lighting, which have been reported before,[16f] as well as the results of control experiments under photoirradiation without Fe^{II}N4Py complexes are also included in Table 2. Under photoirradiation, all five iron(II) complexes investigated induced significantly more DNA cleavage within 90 min compared to those under ambient conditions. Furthermore, DNA cleavage under photoirradiation continued over 90 min, which is in contrast with the experiments under ambient lighting, where the activity was significantly reduced after 60 min.[16f] Under ambient lighting, the iron(II) complexes of ligands **1**−**5** induce ssc only.[16f] Similarly, under irradiation with light of 473 and 400.8 nm, only nicked and supercoiled DNA were present during the reaction. In contrast, under photoirradiation at 355 nm, the formation of 13−19% linear DNA was observed.[24] In the absence of a cleaving agent, DNA cleavage was not observed under photoirradiation at 473 and 400.8 nm; however, at 355 nm, a small degree of DNA cleavage (~16%) was observed (Table 2, entry 1). This is tentatively ascribed to Fenton-like chemistry resulting from traces of metal ions in solution.

It is known that free iron(II) salts and aromatic compounds are capable of inducing DNA cleavage under photoirradiation through Fenton-like chemistry and the formation of ROS.[17] The preparation of the complex in situ raises the possibility that incomplete complexation and thus free ligand and iron salts may be present in the reaction mixture. A series of control experiments were performed with only $(NH_4)_2Fe^{II}(SO_4)_2 \cdot 6H_2O$, only the N4Py ligand **1**, in situ prepared complex, and a preformed complex $[Fe^{II}(N4Py)CH_3CN)](ClO_4)_2$ to assess the activity in DNA cleavage under ambient lighting conditions and continuous photoirradiation at 400.8 nm (1.2 mW) and 355 nm (2.6 mW). The results are listed in Table 3. Under all lighting conditions, the combination of $(NH_4)_2Fe^{II}(SO_4)_2 \cdot 6H_2O$ and ligand **1** showed the same activity as the preformed complex Fe^{II}-**1** within experimental uncertainty (Table 3, entries 3 and 4); in contrast, $(NH_4)_2Fe^{II}(SO_4)_2 \cdot 6H_2O$ or ligand **1** alone induced no significant DNA cleavage under any of the conditions employed. These observations confirm that the activity observed arises from the FeN4Py complex. Control experiments using the free chromophores 9-aminoacridine and 1,8-naphthalimide were

(24) The first term of the Poisson distribution predicts that the amount of linear DNA will reach a maximum at around 37%; in practice, this means that smaller fragments of DNA are produced, and as a result, significant amounts of a smear appear in the gel, which precludes quantitative analysis. For Fe^{II}-**2**, the quantification of linear DNA was not possible because of the extensive DNA cleavage. Also see refs 16d−16f.

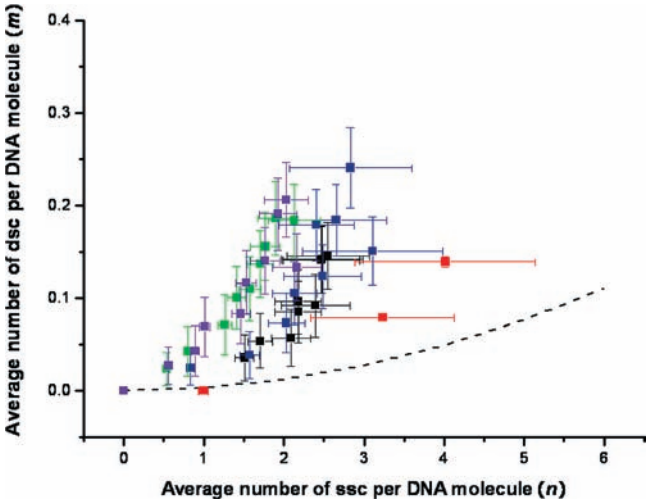

Figure 1. Number of double-strand cuts (m) as a function of the single-strand cuts (n) per DNA molecule for Fe^{II}-**1** (black ■), Fe^{II}-**2** (red ■), Fe^{II}-**3** (blue ■), Fe^{II}-**4** (green ■), and Fe^{II}-**5** (purple ■) under photoirradiation at 355 nm. Error bars represent the maximum and the minimum values of n and m. Dotted lines describe a pure single-strand cleavage pathway, as described by the Freifelder−Trumbo relationship.[22a].

also carried out, in which a significant amount of DNA cleavage was observed with 1,8-naphthalimide under photoirradiation at 355 nm (Table 3, entry 6). This is attributed to photosensitized DNA cleavage involving singlet oxygen.[17] Importantly, at 400.8 nm, no DNA cleavage was observed with 1,8-naphthalimide.

Effect on the DNA Cleavage Pathway. In the case of DNA cleavage under photoirradiation at 473 and 400.8 nm, only nicked DNA was formed and, hence, it can be concluded that only ssc takes place. The formation of linear DNA at 355 nm suggests that a double-strand cleavage pathway may be involved as well. Linear DNA can be produced by direct double-strand cleavage or by extensive single-strand cleavage. To distinguish between these different cleavage pathways, the numbers of single-strand (n) and double-strand (m) cuts per DNA molecule were calculated for all time points by statistical analysis using the Poisson distribution as described before[16d−f] and compared with the Freifelder−Trumbo relationship, which describes a pure single-strand cleavage pathway.[22a] Figure 1 shows the plots of the number of double-strand cleavage (m) versus the number of single-strand cleavage (n) for the iron(II) complexes of ligands **1**−**5** under photoirradiation at 355 nm. The dotted line is the theoretical curve following from the Freifelder−Trumbo relationship. For Fe^{II}-**1**−**5**, the values of m and n increased with time, which is consistent with continued DNA cleavage over 90 min (Figure 1). The m/n plot of complex Fe^{II}-**2** approaches the Freifelder−Trumbo relationship, which suggests this is predominantly a single-strand DNA cleaving agent. In the case of Fe^{II}-**1**, Fe^{II}-**3**, Fe^{II}-**4**, and Fe^{II}-**5**, the m/n plots deviate more strongly from the Freifelder−Trumbo relationship, indicating that, in addition to single-strand cleavage, direct double-strand cleavage occurs also. Furthermore, because the m/n plots of Fe^{II}-**4** and Fe^{II}-**5** deviate more from the Freifelder−Trumbo relationship than Fe^{II}-**1** and Fe^{II}-**3** do, it can be concluded that more direct dsc was induced by the former complexes.

Fe^{II}-**4** is also capable of inducing direct double-strand cleavage in the presence of 1000 equiv of reducing agent DTT.[16f] The comparison of the m/n plots of Fe^{II}-**4** under photoirradiation at 355 nm and with DTT shows that more double-strand cleavage activity was observed under photoirradiation (Figure S7 in the Supporting Information). Another notable observation is that under photoirradiation at 355 nm the m/n plot deviates from the Freifelder−Trumbo relationship from the beginning. This suggests that both dsc and ssc occur from the start of the reaction. In contrast, in the absence of laser excitation and in the presence of DTT, the m/n plot first approximates the Freifelder−Trumbo relationship and later deviates from it, indicating that double-strand cleavage occurs only after a significant amount of nicked DNA has been formed (Figure S7 in the Supporting Information).

Effect on the Cleavage Rate. For DNA cleavage processes involving only single-strand cleavage, the number of single-strand cuts (n) at different time points was calculated and plotted against time to obtain the pseudo-first-order rate constant k_{obs} (Figure S8 and Table S2 in the Supporting Information). The apparent pseudo-first-order rate constant k^*, which is obtained from k_{obs} by taking into account the concentrations of DNA and iron(II) complexes, was used to describe the DNA cleavage efficiency of the complexes.[16f] The values of k^* for DNA cleavage with iron(II) complexes of ligands **1**−**5** under ambient lighting and photoirradiation are listed in Table 4.

With photoirradiation, DNA cleavage processes are significantly faster than those under ambient lighting. The ssc activity of Fe^{II}-**1**−**5** under photoirradiation at 473 nm was significantly higher than that under ambient lighting, and the highest activity was found with Fe^{II}-**2**. Under photoirradiation at 400.8 nm, the k^* values for all complexes are higher than those at 473 nm, and the same trend in k^* was observed for the complexes, i.e., in which the largest value of k^* was obtained with Fe^{II}-**2**. Under photoirradiation at 355 nm, the dsc activity was observed with Fe^{II}-**1** and Fe^{II}-**3**−**5**; therefore, the apparent rate constants were not calculable. Fe^{II}-**2** is the most active complex under photoirradiation at 355 nm, with an increase in k^* from 1.97×10^{-4} min^{-1} under ambient lighting to 1.11×10^{-2} min^{-1}, which corresponds to a 56-fold acceleration of the DNA cleavage process (Table 4, entry 2).

Notably, it was observed that the activity of the parent complex Fe^{II}-**1** is higher than that of the naphthalimide-conjugated complexes Fe^{II}-**3**−**5** under both ambient lighting and photoirradiation, indicating that the naphthalimide moiety does not contribute favorably to the DNA cleavage activity. The ssc activity of Fe^{II}-**5**, with two covalently appended 1,8-naphthalimide moieties, is significantly smaller than that of Fe^{II}-**3** and Fe^{II}-**4** under photoirradiation at 473 and 400.8 nm, strongly suggesting an important negative influence of the second 1,8-naphthalimide moiety.

In order to gain insight into the lower activity found for the naphthalimide-derived ligands, optical measurements were performed for ligands **3**−**5** and their corresponding iron(II) complexes. The fluorescence response of **3**−**5** upon the addition of 1 equiv of Fe^{2+} was investigated in 10 mM Tris-HCl buffer (pH 8.0) at 20 °C (Figure S9 in the Supporting Information). For ligands **3** and **4**, the addition of Fe^{2+} caused a significant decrease in the fluorescence

Table 4. Rate Constants of DNA Cleavage (k^*) under Ambient Lighting and Photoirradiation[a]

		cleavage rate k^* (10^{-3} min^{-1})			
entry	complex	ambient lighting	473 nm (30.3 mW)	400.8 nm (17.4 mW)	355 nm (24.6 mW)
1	Fe^{II}-**1**	0.197 ± 0.017[b]	0.372 ± 0.034	0.519 ± 0.056	*d*
2	Fe^{II}-**2**	0.197 ± 0.006	0.474 ± 0.011	0.998 ± 0.034	11.1 ± 0.85[e]
3	Fe^{II}-**3**	0.158 ± 0.011[b]	0.243 ± 0.011	0.248 ± 0.017	*d*
4	Fe^{II}-**4**	*c*	0.259 ± 0.023	0.321 ± 0.028	*d*
5	Fe^{II}-**5**	*c*	0.051 ± 0.006	0.090 ± 0.006	*d*

[a] 1 μM iron complex, 0.1 $\mu g\,\mu L^{-1}$ supercoiled pUC18 DNA (150 μM bp), Tris-HCl buffer (pH 8.0), 37 °C. A correction factor of 1.31 was used to compensate for the reduced EtBr uptake capacity of supercoiled plasmid pUC18 DNA.[16d] [b] The cleavage rate was obtained within 60 min.[16f] [c] The cleavage rate cannot be obtained through the small numbers of single-strand cuts (n).[16f] [d] The cleavage rate cannot be obtained because a double-strand cleavage pathway is involved. [e] The cleavage rate was obtained within 60 min, which is before the DNA cleavage process reaches the limit of accurate quantification.

Table 5. Quantum Yields of Emission of Fluorophore-Attached Ligands and Their Iron(II) Complexes

ligand	Φ_f	Fe^{II}-ligand	Φ_f
3	0.094	Fe^{II}-**3**	0.079
4	0.084	Fe^{II}-**4**	0.027
5	0.018	Fe^{II}-**5**	0.0055

emission intensity, which suggests electron and/or energy transfer between the photoexcited fluorophore, i.e., naphthalimide, and the iron center bound to N4Py. A higher degree of quenching of the fluorescence emission was observed with **4** containing a longer linker, indicating a stronger interaction. This is most likely the result of the higher structural flexibility of Fe^{II}-**4**, which facilitates interaction between the iron(II) center and the naphthalimide. As a result, both are less available for interaction with the DNA, resulting in a lower DNA cleavage activity. As mentioned above, the UV−vis absorption spectra suggested that aggregates of Fe^{II}-**5** were formed in aqueous solution even at low concentrations (Figure S3 in the Supporting Information). In agreement with this observation, an excimer emission was observed for both free ligand **5** and complex Fe^{II}-**5**. The quantum yields (Φ_f) of fluorescence of ligands **3**−**5** and complex Fe^{II}-**3**−**5** are listed in Table 5. Photoinduced electron and/or energy transfer between the excited naphthalimide and the iron center may account for the decrease in the Φ_f values of Fe^{II}-**3**−**5** compared to those of ligands **3**−**5**. The observed aggregation of Fe^{II}-**5** is most likely the cause of the lower DNA cleavage activity.

Power Dependence of the Photoirradiation Effect. The power dependence of the DNA cleavage activity of Fe-**2**, which is the most active complex in the study described above, was investigated at 355 nm using a CW laser with a light flux of 5.2×10^{15} photons s^{-1} (2.9 mW) and pulsed lasers with a light flux of 5.7×10^{15} photons s^{-1} (3.2 mW) and 4.4×10^{16} photons s^{-1} (24.6 mW). Figure 2 shows the average numbers of single-strand cuts (n) of Fe-**2** at 30 min. A similar DNA cleavage activity was observed with the CW and pulsed lasers at similar light flux, with n of 0.899 ± 0.054 and 0.898 ± 0.050, respectively. This suggests that pulsed and continuous irradiation at the same power affect the DNA cleavage processes comparably. The increase in the DNA cleavage activity observed with the pulsed laser at 355 nm with a light flux of 4.4×10^{16} photons s^{-1} (24.6 mW) demonstrates that the cleavage process is approximately linearly dependent on the irradiation power.

Mechanistic Investigation. The nature of the ROS involved in the photoenhanced DNA cleavage was investigated

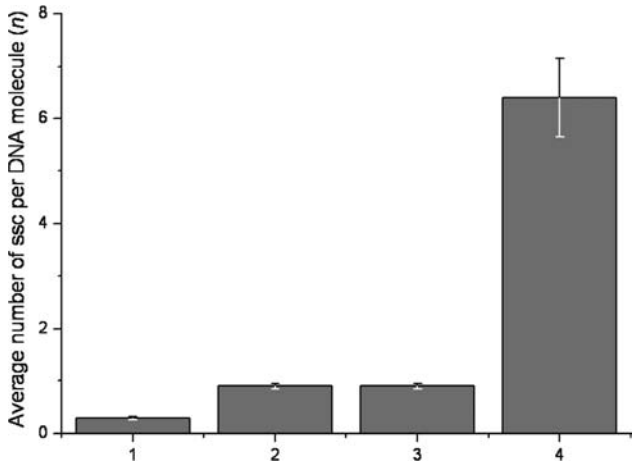

Figure 2. Calculated average numbers of single-strand cuts per DNA molecule (n) of Fe-**2** at 30 min: (1) under ambient lighting; (2) CW laser 355 nm (2.9 mW); (3) pulsed laser 355 nm (3.2 mW); (4) pulsed laser 355 nm (24.6 mW).

by the addition of a series of mechanistic probes. The ROS scavengers that were used include NaN_3, which is a known singlet oxygen ($^1O_2$) scavenger,[25] dimethyl sulfoxide (DMSO), which acts as a hydroxyl radical scavenger,[26] SOD, which converts superoxide radicals into O_2 and H_2O_2,[27] and catalase, which converts H_2O_2 into O_2 and H_2O.[28] These investigations were focused on the parent complex Fe^{II}-**1**. With complexes Fe^{II}-**2**−**5**, which are more strongly bound to DNA because of the covalently attached DNA binding moiety, it may be difficult to intercept any ROS with a scavenger before DNA damage occurs, which would potentially skew mechanistic conclusions.

Table S3 and Figure S10 in the Supporting Information and Figure 3 show the average numbers of single-strand cuts (n) of Fe-**1** with different scavengers at 30 min under ambient lighting and photoirradiation at 473, 400.8, and 355 nm, respectively. As reported before, the activity of Fe^{II}-**1** under ambient lighting involves superoxide radicals.[16f]

(25) Hasty, N.; Merkel, P. B.; Radlick, P.; Kearns, D. R. *Tetrahedron Lett*. **1972**, *1*, 49–52.
(26) Repine, J. E.; Pfenninger, O. W.; Talmage, D. W.; Berger, E. M.; Pettijohn, D. E. *Proc. Natl. Acad. Sci. U.S.A*. **1981**, *78*, 1001–1003.
(27) (a) McCord, J. M.; Fridovic, I. *J. Biol. Chem*. **1969**, *244*, 6049–6055. (b) Lah, M. S.; Dixon, M. M.; Pattridge, K. A.; Stallings, W. C.; Fee, J. A.; Ludwig, M. L. *Biochemistry* **1995**, *34*, 1646–1660. (c) Dismukes, G. C. *Chem. Rev*. **1996**, *96*, 2909–2926. (d) Vance, C. K.; Miller, A. F. *Biochemistry* **2001**, *40*, 13079–13087.
(28) Wu, A. J.; Penner-Hahn, J. E.; Pecoraro, V. L. *Chem. Rev*. **2004**, *104*, 903–938.

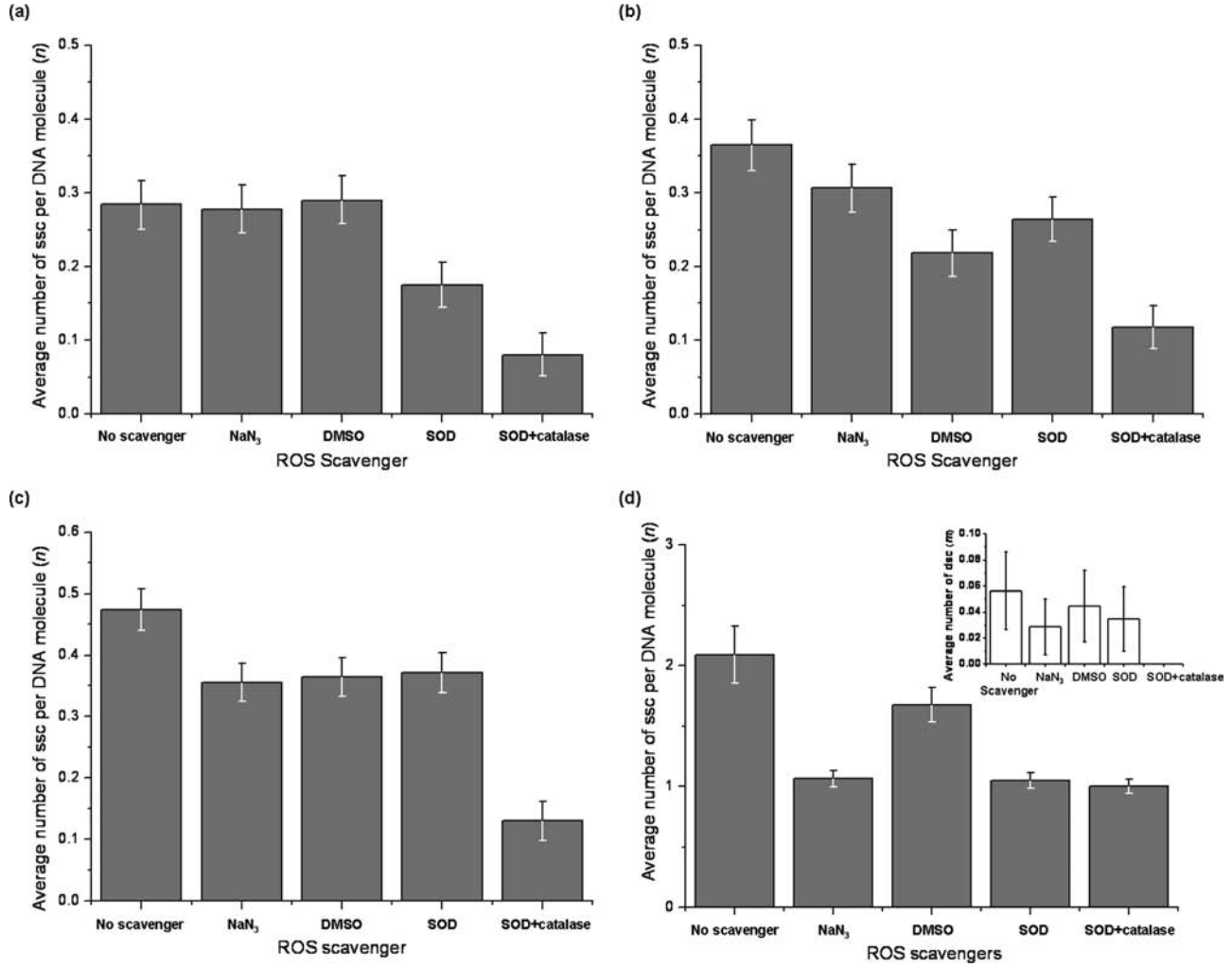

Figure 3. Calculated average numbers of single-strand cuts per DNA molecule (n) of Fe-**1** at 30 min with ROS scavengers: (a) under ambient lighting; (b) 473 nm (CW laser, 30.3 mW); (c) 400.8 nm (CW laser, 17.4 mW); (d) 355 nm (pulsed laser, 24.6 mW). Inset: numbers of double-strand cuts (m).

As a consequence, the DNA cleavage activity is not affected by the presence of NaN_3 and DMSO but is significantly reduced by the presence of SOD and SOD in combination with catalase.[16f] Under photoirradiation, the DNA cleavage efficacy of Fe-**1** was inhibited by all scavengers, albeit to various extents and depending on the wavelength used. This suggests that the observed activity results from multiple ROS, e.g., $^1O_2$, $OH^\bullet$, and $O_2^{\bullet-}$, which is in marked contrast with Fe-**1** under ambient lighting.

Under photoirradiation at 473 nm, a small decrease in the single-strand cleavage activity of Fe-**1** was observed by the addition of NaN_3 (~16%) and SOD (~18%). The addition of DMSO resulted in a moderate drop (~40%) in the activity. A strong inhibition (~68%) was observed upon the addition of SOD and catalase together (Table S3 in the Supporting Information and Figure 3b). A similar pattern was observed when 400.8 nm light was employed. The addition of NaN_3, DMSO, and SOD gave rise to a small decrease (~20%) in the activity, respectively, and the addition of SOD and catalase together resulted in a strong decrease in the activity (~73%) (Table S3 in the Supporting Information and Figure 3c). At 355 nm, the addition of NaN_3, SOD, and SOD combined with catalase resulted in a moderate drop (~40%) in the single-strand cleavage activity of Fe-**1**, while the addition of DMSO resulted in a smaller extent of inhibition (~20%) (Table S3 in the Supporting Information and Figure 3d). Interestingly, in the case where SOD and catalase were added together, dsc was inhibited completely (Figure 3d, inset). These results demonstrate that the contribution of the different ROS, i.e., $^1O_2$, $OH^\bullet$, and $O_2^{\bullet-}$, to the total activity of Fe^{II}-**1** under photoirradiation, is dependent on the conditions of photoirradiation and that $O_2^{\bullet-}$ is of particular importance for the observed activity.

Fe^{II}N4Py under Photoirradiation. Notably, it was observed that the parent Fe^{II}N4Py complex, Fe^{II}-**1**, without appended chromophores, already displays significantly enhanced DNA cleavage activity under photoirradiation. Marked differences were observed in the DNA cleavage with Fe^{II}-**1**, depending on the wavelength used for photoirradiation. Considerably more DNA cleavage was found under photoirradiation generated with a pulsed laser at 355 nm compared to the CW laser at 473 and 400.8 nm. This can be attributed only partly to an increased light-induced background reaction at 355 nm, which does not occur at 473 and 400.8 nm (Table 2, entry 1). Furthermore, under irradiation at 355 nm, also direct double-strand cleavage was observed, whereas at 473 and 400.8 nm, pure single-strand cleavage was observed. These results suggest that, by irradiation with 355 nm, a wide range of ROS may be generated compared to irradiation at longer

wavelengths. Indeed, the mechanistic probes employed also resulted in different inhibition patterns depending on the wavelength used.

At all wavelengths investigated, SOD combined with catalase generally gave rise to the most significant degree of inhibition, suggesting that, also under photoirradiation, $O_2^{\bullet-}$ is the dominant contributor to the DNA cleavage activity of Fe^{II}-**1**. This is similar to what was found for the cleavage reaction under ambient lighting.[16f] However, under photoirradiation, inhibition is also observed to a variable extent with the other ROS scavengers employed, which is in contrast with the cleavage reactions under ambient lighting. The inhibition pattern observed in the case of irradiation at 355 nm is in stark contrast with that observed at 473 and 400.8 nm. At 355 nm in particular, significant inhibition is observed upon the addition of NaN_3, which indicates the involvement of singlet oxygen. To a lesser extent, inhibition by DMSO is observed, which could be indicative of the involvement of $OH^{\bullet}$.

There are several possible rationalizations for the significant effect of photoirradiation on DNA cleavage with Fe^{II}-**1**. Because at higher irradiation wavelengths superoxide radicals are the dominant contributors to the observed DNA cleavage activity, it can be assumed that electron-transfer processes, resulting in the reduction of O_2 to $O_2^{\bullet-}$, play an important role. Superoxide radicals were also proposed as the key species involved in the Fe^{II}-**1**-mediated DNA cleavage under ambient lighting.[16f] Therefore, this suggests that while photoirradation leads to a more efficient DNA cleavage process, it does not fundamentally alter the DNA cleavage chemistry. Our hypothesis is that photoinduced spin-crossover transitions following metal-to-ligand-charge-transfer (MLCT) excitation[29] yield high-spin-state iron(II) complexes that can engage in electron transfer to O_2. This step is the key to the observed increase in the DNA cleavage activity. Alternatively, light-induced dissociation of a coordinated solvent molecule to generate a vacant coordination site, accompanied by a low-spin to a high-spin transition, would generate a species capable of reacting with O_2 to generate superoxide radicals or that will react with superoxide to produce the active $Fe^{III}OOH$ intermediate.[16f] This is analogous to earlier reports in which photoexcitation at 355 nm in the presence of O_2 resulted in dissociation of carbon monoxide from $[Cu^{I}(tmpa)(CO)]^{+}$ via a MLCT state $[Cu^{I}(d_{10})-N_{py}(\pi^*)]$ and subsequent formation of a cupric superoxo ($Cu^{II}O_2^{\bullet-}$) species.[30]

At 355 nm, more than one ROS were demonstrated to be involved in DNA cleavage. Therefore, it is likely that in this case more than one light-induced process is contributing to the overall activity. In addition to the processes that result in the formation of superoxide, as described above, it is likely that the photosensitized generation of $^1O_2$ is also involved. This could occur through ligand-based photosensitized generation of $^3O_2$.[18d,31] It has been reported that photogenerated $^1O_2$ is mainly affecting the oxidation of DNA nucleobases, preferentially guanines, rather than the cleavage of phosphate−deoxyribose backbones.[32,33]

Photogeneration of $OH^{\bullet}$ can also promote DNA cleavage because $OH^{\bullet}$ is an intermediate reactive species capable of abstracting hydrogen atoms from the deoxyribose moieties of DNA. The resultant sugar radicals are known to result in base release and associated ssc.[11,18g,33,34] The involvement of $OH^{\bullet}$ in DNA cleavage with Fe^{II}-**1** under photoirradiation was observed, however, albeit only to a minor extent. Furthermore, it should be noted that homolytic scission of the O−O bond in $N4PyFe^{III}OOH$, which is proposed to be the active species or precursor for DNA cleavage, probably will result in the formation of $OH^{\bullet}$ and $N4PyFe^{IV}=O$.[35]

Chromophore-Attached Fe^{II}N4Py under Photoirradiation. Fe^{II}-**2**, which contains a covalently attached 9-aminoacridine moiety, exhibited higher activity than Fe^{II}-**1** under photoirradiation. Acridine derivatives and analogues such as acridine orange and proflavin are capable of photocleavaging DNA through the generation of $O_2^{\bullet-}$ and $^1O_2$.[36] Furthermore, the photoreduction of Fe^{III} to Fe^{II} can be effected by electron transfer from the photochemically excited triplet states of acridine orange, proflavin, and other 3,6-acridinediamines.[20c,37,38] Therefore, it is hypothesized that the higher activity of Fe^{II}-**2** results from a combination of acridine-sensitized generation of $O_2^{\bullet-}$ and photoreduction of Fe^{III} back to Fe^{II}, which can then engage in another DNA cleavage event. Combined, these processes should dramatically increase the formation of the active oxidant $N4PyFe^{III}OOH$. Additionally, the strong DNA binding affinity provided by the 9-aminoacridine moiety is also expected to contribute favorably to the observed DNA cleavage activity, as was reported before.[16b,f] Finally, electron transfer from the DNA nucleobases, especially guanines, to the photoexcited 9-aminoacridine moiety may further increase its electron-donor ability.[18g]

For Fe^{II}-**3**−**5**, which contain 1,8-naphthalimide moieties, it has been proposed that interaction between the Fe^{II}-N4Py core and naphthalimide accounts for their lower activity. Indeed, naphthalimides are well-known model acceptors for photoinduced electron transfer in photophysical studies.[17f,39] Therefore, intramolecular electron transfer from the iron(II) center to the naphthalimide moieties may compete with the reduction of O_2 to $O_2^{\bullet-}$, resulting in the formation of iron(III) species and thereby reducing the activity.

(29) (a) Decurtins, S.; Gütlich, P.; Köhler, C. P.; Spiering, H.; Hauser, A. *Chem. Phys. Lett*. **1984**, *105*, 1–4. (b) Hauser, A.; Gütlich, P.; Spiering, H. *Inorg. Chem*. **1986**, *25*, 4245–4248. (c) Toftlund, H. *Monatsh. Chem*. **2001**, *132*, 1269–1277. (d) Brady, C.; Callaghan, P. L.; Ciunik, Z.; Coates, C. G.; Dossing, A.; Hazell, A.; McGarvey, J. J.; Schenker, S.; Toftlund, H.; Trautwein, A. X.; Winkler, H.; Wolny, J. A. *Inorg. Chem*. **2004**, *43*, 4289–4299.

(30) Fry, H. C.; Scaltrito, D. V.; Karlin, K. D.; Meyer, G. J. *J. Am. Chem. Soc*. **2003**, *125*, 11866–11871.

(31) (a) Foote, C. S. *Acc. Chem. Res*. **1968**, *1*, 104–110. (b) Kearns, D. R. *Chem. Rev*. **1971**, *71*, 395–427. (c) McClain, W. M. *Acc. Chem. Res*. **1974**, *7*, 129–135. (d) Schweitzer, C.; Schmidt, R. *Chem. Rev*. **2003**, *103*, 1685–1758. (e) Celli, J. P.; Spring, B. Q.; Rizvi, I.; Evans, C. L.; Samkoe, K. S.; Verma, S.; Pogue, B. W.; Hasan, T. *Chem. Rev*. **2010**, *110*, 2795–2838.

(32) Meunier, B.; Pratviel, G.; Bernadou, J. *Bull. Soc. Chim. Fr*. **1994**, *131*, 933–943.

(33) Burrows, C. J.; Muller, J. G. *Chem. Rev*. **1998**, *98*, 1109–1152.

(34) Adhikary, A.; Kumar, A.; Sevilla, M. D. *Radiat. Res*. **2006**, *165*, 479–484.

(35) Roelfes, G.; Lubben, M.; Hage, R.; Que, L., Jr.; Feringa, B. L. *Chem.—Eur. J*. **2000**, *6*, 2152–2159.

(36) (a) Freifelder, D.; Davison, P. F.; Geiduschek, E. P. *Biophys. J*. **1961**, *1*, 389–400. (b) Piette, J.; Calberg-Bacq, C. M.; van de Vorst, A. *Photochem. Photobiol*. **1979**, *30*, 369–378. (c) Piette, J.; Lopez, M.; Calberg-Bacq, C. M.; van de Vorst, A. *Int. J. Radiat. Biol*. **1981**, *40*, 427–433. (d) Bowler, B. E.; Hollis, S.; Lippard, S. J. *J. Am. Chem. Soc*. **1984**, *106*, 6102–6104.

(37) Oster, G. K.; Oster, G. *J. Am. Chem. Soc*. **1959**, *81*, 5543–5545.

(38) Kellmann, A. *Photochem. Photobiol*. **1974**, *20*, 103–108.

Table 6. Iron Complexes Capable of Photoactivated DNA Cleavage[a]

no.	complex	proposed reactive species	ratio of iron to DNA bp	excitation wavelength (nm)	ref
1	$Fe^{III}\cdot 3L_1$	$L_1^{\bullet}$	10:1	≥400	20a
2	$CpFe^{II}(CO)_2R$ (R = CH_3, C_6H_5)	$R^{\bullet}$	0.09:1	200−600	20b
3	$Fe^{III}\cdot L_2$	$OH^{\bullet}$, $O_2^{\bullet-}$	0.33:1	low-intensity visible light	20c
4	$[Fe^{II}(L_3)(L_4)](PF_6)_3$	$^1O_2$	not reported	312, 365	20d
5	$[\{Fe^{III}$(L-histidine)(B)$\}_2(\mu$-O)$](ClO_4)_2$	$OH^{\bullet}$	0.17:1, 1.3:1	365, 458, 520, 647	20e
6	$Fe^{III}(B)L_5$	$OH^{\bullet}$	0.17:1, 1:1	365, 476, 514, 532, 568, 647,	20f
7	$[Fe^{III}(L_6)_2]Cl$	$OH^{\bullet}$	3.3:1, 1.6:1	365, 476, 514, 633	20g
8	Fe^{II}N4Py complexes	$^1O_2$, $OH^{\bullet}$, $O_2^{\bullet-}$, N4PyFe^{III}OOH	0.007:1	355, 400.8, 473	this work

[a] L_1 = 3-hydroxy-1,2,3-benzotriazine-4(3*H*)-one; L_2 = *N*,*N*′-bis[2-[bis(1*H*-imidazol-4-ylmethyl)amino]ethyl]-3,6-acridinediamine; for L_3 and L_4, see ref 20d; B = 1,10-phenanthroline (phen), dipyridoquinoxaline (dpq), and dipyridophenazine (dppz); L_5 = 2-bis[3,5-di-*tert*-butyl-2-hydroxybenzyl]aminoacetic acid; L_6 = *N*-salicylidenearginine, hydroxynaphthylidenearginine, and *N*-salicylidenelysine.

Comparison with Other Photoactive Iron Complexes. A variety of iron complexes capable of DNA cleavage under photoirradiation have been reported and are summarized in Table 6. $O_2^{\bullet-}$ was also found to be the key intermediate in photoirradiated DNA cleavage induced with an iron(III) complex of the acridine−imidazole conjugate (Table 6, entry 3); however, further discussions on the reaction mechanism and reactive species were not provided.[20c] For the other iron complexes that have been employed in photoinduced DNA cleavage, ligand-localized radicals[20a,b] and $OH^{\bullet}$[20e−g] were proposed to be the dominant reactive intermediates. The present N4Py-derived iron(II) complexes are different from the reported examples in the literature in that Fe^{II}N4Py complexes are already active in DNA cleavage without photoirradiation. Depending on the light source, photoirradiation significantly enhanced the cleaving activity of Fe^{II}N4Py complexes, in which $^1O_2$ and $OH^{\bullet}$ are involved but the dominant ROS species is $O_2^{\bullet-}$. These may give rise to the formation of N4Py-Fe^{III}OOH species, which are proposed to be the active species or precursor in the DNA cleavage process.[16f]

Conclusions

The photoirradiation of iron(II) complexes of monotopic N4Py ligands **1**−**5** at 473, 400.8, and 355 nm induced significantly increased DNA cleavage activity under aerobic conditions without any external reducing agent. The characteristics of the observed activity of these mononuclear Fe^{II}N4Py complexes depended strongly on their structures and, in particular, on the chromophores that were covalently attached to the N4Py ligand. The parent Fe^{II}N4Py complex, Fe^{II}-**1**, which does not contain covalently appended chromophores, already displays significantly enhanced DNA cleavage activity under photoirradiation. Interestingly, the order of activity was found to be Fe^{II}-**2** > Fe^{II}-**1** > Fe^{II}-**3**−**5** under all of the photoirradiation conditions employed in the study, where a covalently linked 9-aminoacridine moiety led to increased activity but covalently attached 1,8-naphthalimide moieties resulted in less efficient activity compared to the parent complex Fe^{II}-**1**. The lower activity of the complexes containing naphthalimide moieties was attributed to interaction of the iron(II) center and the naphthalimide. The difference between the electronic properties of 9-aminoacridine and 1,8-naphthalimide is likely to influence the reduction of Fe^{III}N4Py back to Fe^{II}N4Py via photoinduced intramolecular electron transfer, and thus effect the DNA cleavage activity.

With CW photoirradiation at 473 nm (30.3 mW) and 400.8 nm (17.4 mW), Fe^{II}-**1**−**5** effected significantly enhanced ssc compared to ambient lighting conditions. With pulsed irradiation at 355 nm (24.6 mW), the enhancement of the activity is more pronounced, which is attributed to the coinvolvement of other ROS that are photochemically generated. In some cases at 355 nm, this resulted in direct dsc in addition to ssc.

Inhibition experiments with different ROS scavengers and Fe^{II}-**1** demonstrated that $^1O_2$, $OH^{\bullet}$, and $O_2^{\bullet-}$ contribute to the total DNA cleavage activity to different extents depending on the wavelength used. In all cases, $O_2^{\bullet-}$ plays a dominant role. It is proposed that $O_2^{\bullet-}$ reacts with the iron(II) complexes to give of the active species or precursor, most likely iron(III) peroxo and/or iron(III) hydroperoxide complexes. For the DNA cleavage process under ambient lighting, the same species were proposed to be involved. Therefore, it is concluded that the mechanism of the DNA cleavage process itself is not changed by photoirradiation.[16f] Rather the higher activity under photoirradiation is due to the increased rate of production of ROS, in particular $O_2^{\bullet-}$. The detailed origin of the photoactivation of Fe^{II}N4Py complexes in DNA cleavage is currently under investigation. Importantly, the significant enhancement of the DNA cleavage activity of Fe^{II}-**1**−**5** under photoirradiation at 473 and 400.8 nm suggests that enhanced activity of Fe^{II}N4Py complexes at wavelengths of 600−800 nm is feasible via two-photon excitation, which is of potential interest for the development of metal-based DNA cleaving agents in photodynamic therapy.[18d,31e]

Acknowledgment. We thank Dr. J. Wang for assistance with determination of the irradiation power. Financial support from the University of Groningen, and Netherlands Organization for Scientific Research (NWO) is gratefully acknowledged.

Supporting Information Available: Experimental setup, determination of the irradiation power, graphs of the DNA cleavage time trace and single-strand cuts (*n*) for Fe^{II}-**1**−**5** under photoirradiation, table of k_{obs} for Fe^{II}-**1**−**5**, and the mechanistic investigation on Fe^{II}-**1**. This material is available free of charge via the Internet at http://pubs.acs.org.

(39) For examples, see:(a) De Silva, A. P.; Gunaratne, H. Q. N.; Habib-Jiwan, J.; McCoy, C. P.; Rice, T. E.; Soumillion, J. *Angew. Chem., Int. Ed. Engl.* **1995**, *34*, 1728–1731. (b) van Dijk, S. I.; Groen, C. P.; Hartl, F.; Brouwer, A. M.; Verhoeven, J. W. *J. Am. Chem. Soc.* **1996**, *118*, 8425–8432. (c) Kawai, K.; Osakada, Y.; Takada, T.; Fujitsuka, M.; Majima, T. *J. Am. Chem. Soc.* **2004**, *126*, 12843–12846. (d) Thompson, A. L.; Ahn, T.-S.; Justin Thomas, K. R.; Thayumanavan, S.; Martínez, T. J.; Bardeen, C. J. *J. Am. Chem. Soc.* **2005**, *127*, 16348–16349.